

Faddeev calculations of the $\bar{K}NN$ system with a chirally motivated $\bar{K}N$ interaction.

I. Low-energy K^-d scattering and antikaonic deuterium

N. V. Shevchenko^{1,*} and J. Révai²¹*Nuclear Physics Institute, 25068 Řež, Czech Republic*²*Wigner Research Center for Physics, RMI, P.O. Box 49, H-1525 Budapest, Hungary*

(Received 4 March 2014; revised manuscript received 17 April 2014; published 25 September 2014)

A chirally-motivated coupled-channel $\bar{K}N$ potential, reproducing all low-energy experimental data on K^-p scattering and kaonic hydrogen and suitable for using in accurate few-body calculations, was constructed. The potential was used for calculations of low-energy amplitudes of elastic K^-d scattering using Faddeev-type Alt-Grassberger-Sandhas (AGS) equations with coupled $\bar{K}NN$ and $\pi\Sigma N$ channels. A complex $K^- - d$ potential reproducing the three-body K^-d amplitudes was constructed and used for calculation of the $1s$ level shift and the width of kaonic deuterium. The predicted shift $\Delta E_{1s}^{K^-d} \sim -830$ eV and width $\Gamma_{1s}^{K^-d} \approx 1055$ eV are close to our previous results obtained with phenomenological $\bar{K}N$ potentials. No quasi-bound states in the K^-d system were found.

DOI: [10.1103/PhysRevC.90.034003](https://doi.org/10.1103/PhysRevC.90.034003)

PACS number(s): 13.75.Jz, 11.80.Gw, 24.10.Eq, 36.10.Gv

I. INTRODUCTION

Interaction of an antikaon with a nucleon is the basis for investigation of atomic and strong quasi-bound states in antikaonic-nucleus systems. Available two-body experimental information on the $\bar{K}N$ interaction is insufficient for construction of a unique interaction model. In particular, it was shown in [1,2] that phenomenological models of the interaction having one or two poles for the $\Lambda(1405)$ resonance reproducing all low-energy experimental data on K^-p scattering and kaonic hydrogen equally well can be constructed. A way to obtain some additional information about the $\bar{K}N$ interaction is to use it as an input in an accurate few-body calculation and then compare the theoretical predictions with eventual experimental data.

There are several calculations devoted to low-energy K^-d scattering [3,4] or the K^-d scattering length only [5,6] based on Faddeev equations. Low-energy K^-d amplitudes, including scattering length, and effective range were calculated in our papers [1,2]. In the most recent one [2] the directly measurable characteristics of the $1s$ level of kaonic deuterium were calculated as well. This allows a direct comparison of the theoretical predictions with eventual experimental data on kaonic deuterium, which hopefully will be obtained in the SIDDHARTA-2 experiment [7].

The results were obtained by solving coupled-channel Faddeev-type Alt-Grassberger-Sandhas (AGS) equations with phenomenological $\bar{K}N$ potentials. However, many other authors of $\bar{K}N$ interaction models use not a phenomenological, but a chirally-motivated potential, where a $\bar{K}N$ amplitude obtained from a chiral Lagrangian is used as a potential to determine the position of the poles of the $\Lambda(1405)$ resonance. Bethe-Salpeter or Lippmann-Schwinger equations are used for this task. There are quite a few such chirally-motivated potentials available; however, none of them is suited for use in Faddeev calculations since either they have too many coupled channels and cannot be used as is or they are not as accurate in

reproducing experimental data as one would wish. Therefore, we decided to construct a new chirally-motivated model of the $\bar{K}N$ interaction that can be used in dynamically accurate three-body calculations.

The potential reproduces the low-energy data on K^-p scattering and kaonic hydrogen with the same level of accuracy as our previously constructed phenomenological $\bar{K}N$ potentials. We repeated our calculation of low-energy K^-d elastic scattering and the characteristics of kaonic deuterium using the new model of the $\bar{K}N$ interaction and compared the new results with those obtained using phenomenological $\bar{K}N$ potentials. Since the three-body AGS equations and the rest of the two-body input are the same in both calculations, we could isolate the pure effect of the different types of $\bar{K}N$ interaction models.

The description of the chirally-motivated potential is given in the next section. The results on low-energy K^-d scattering are given and discussed in Sec. III. Section IV contains information on the evaluation of the kaonic deuterium $1s$ level shift and width, while Sec. V concludes the paper.

II. CHIRALLY-MOTIVATED $\bar{K}N-\pi\Sigma-\pi\Lambda$ POTENTIAL

There are many different chirally-motivated models of the $\bar{K}N$ interaction in the literature (e.g., [8–10]). Most of them are not really suited for use in Faddeev calculations since they have too many coupled channels. Recently, one more of these $\bar{K}N$ potentials was constructed [11] together with a reduced version, which contains only three channels. Therefore, this last one, in principle, could be used in a dynamically correct few-body calculation; however, the reduced version does not reproduce K^-p experimental data accurately enough.

The commonly used s -wave chirally-motivated potentials have the energy-dependent part (see, e.g., [9])

$$\bar{V}^{ab}(\sqrt{s}) = \sqrt{\frac{M_a}{2\omega_a E_a}} \frac{C^{ab}(\sqrt{s})}{(2\pi)^3 f_a f_b} \sqrt{\frac{M_b}{2\omega_b E_b}} \quad (1)$$

and are written in the particle basis. We took into account all open particle channels: $a, b = K^-p, \bar{K}^0n, \pi^+\Sigma^-, \pi^0\Sigma^0,$

*Corresponding author: shevchenko@ujf.cas.cz

$\pi^- \Sigma^+$, and $\pi^0 \Lambda$. Baryon mass M_a , baryon energy E_a , and meson energy w_a of the channel a enter the factors, which ensure the proper normalization of the amplitude. The nonrelativistic form of the leading order Weinberg-Tomozawa interaction

$$C^{ab}(\sqrt{s}) = -C^{WT} (2\sqrt{s} - M_a - M_b) \quad (2)$$

was used with SU(3) Clebsh-Gordan coefficients C_I^{WT} .

Our chirally-motivated potential $V_{\bar{K}N-\pi\Sigma-\pi\Lambda}^{\text{Chiral}}$ is separable; it also contains form factors and is written in the isospin basis as

$$V_{I I'}^{\alpha\beta}(k^\alpha, k'^\beta; \sqrt{s}) = g_I^\alpha(k^\alpha) \bar{V}_{I I'}^{\alpha\beta}(\sqrt{s}) g_{I'}^\beta(k'^\beta), \quad (3)$$

where $V_{I I'}^{\alpha\beta}(\sqrt{s})$ is the energy-dependent part of the potential in the isospin basis, obtained from Eq. (1). Here k^α , k'^α , and \sqrt{s} stand for the initial and final relative momenta and the total energy, respectively. We used physical masses in the calculations; therefore the two-body isospin $I = 0$ or 1 is not conserved. Yamaguchi form factors

$$g_I^\alpha(k^\alpha) = \frac{(\beta_I^\alpha)^2}{(k^\alpha)^2 + (\beta_I^\alpha)^2} \quad (4)$$

were used in Eq. (3). The channel indices α and β take three values, denoting the $\bar{K}N$, $\pi\Sigma$, and $\pi\Lambda$ channels.

The pseudo-scalar meson decay constants f_π and f_K and the range parameters β_I^α , depending on the two-body isospin, are free parameters found by fitting the potential to the experimental data. In the same way as the phenomenological ones, the potential (3) reproduces elastic and inelastic K^-p cross sections, threshold branching ratios γ , R_c , and R_n , and characteristics of the $1s$ level of kaonic hydrogen. The parameters of the potential are shown in Table I. It has to be noted that our value of f_π , obtained from the fit, differs from the one usually cited in the literature. However, we call our potential ‘‘chirally motivated,’’ and not ‘‘chiral’’ in a sense that certain features of the chiral interaction are preserved (energy dependence, relative coupling strength of channels, and relativistic normalization), while others are not. Our main aim was to construct a potential reproducing all experimental data on K^-p scattering and kaonic hydrogen as accurately as possible.

All physical observables to be compared with experimental data were obtained from solution of the Lippmann-Schwinger equation with the potential $V_{\bar{K}N-\pi\Sigma-\pi\Lambda}^{\text{Chiral}}$ (3) and Coulomb interaction since, as previously, we wanted to calculate characteristics of kaonic hydrogen directly, without intermediate reference to K^-p scattering length. We used nonrelativistic kinematics while the potential was constructed. Among all authors of $\bar{K}N$ potentials only we and Cieplý and Smejkal [9,12] take Coulomb interaction into account directly when calculating the $1s$ level shift and width of kaonic

TABLE I. Parameters of the chirally-motivated $V_{\bar{K}N-\pi\Sigma-\pi\Lambda}^{\text{Chiral}}$ potential: the pseudo-scalar meson decay constants f_π and f_K (in MeV) and the range parameters β_I^α (in fm $^{-1}$).

f_π	f_K	$\beta_0^{\bar{K}N}$	$\beta_0^{\pi\Sigma}$	$\beta_1^{\bar{K}N}$	$\beta_1^{\pi\Sigma}$	$\beta_1^{\pi\Lambda}$
116.20	113.36	4.06	3.30	5.00	3.86	1.99

TABLE II. Physical characteristics of the chirally-motivated $V_{\bar{K}N-\pi\Sigma-\pi\Lambda}^{\text{Chiral}}$ potential [$1s$ level shift $\Delta E_{1s}^{K^-p}$ (in eV) and width $\Gamma_{1s}^{K^-p}$ (in eV) of kaonic hydrogen, and threshold branching ratios γ , R_c , and R_n], together with experimental data. The experimental data on kaonic hydrogen are those obtained by the SIDDHARTA Collaboration.

	$V_{\bar{K}N-\pi\Sigma-\pi\Lambda}^{\text{Chiral}}$	Experiment
$\Delta E_{1s}^{K^-p}$	-313	$-283 \pm 36 \pm 6$ [15]
$\Gamma_{1s}^{K^-p}$	561	$541 \pm 89 \pm 22$ [15]
γ	2.35	2.36 ± 0.04 [16,17]
R_c	0.663	0.664 ± 0.011 [16,17]
R_n	0.191	0.189 ± 0.015 [16,17]

hydrogen. All other calculations of the same quantity get it from the K^-p scattering length through the approximate ‘‘corrected Deser’’ formula [13]. However, as shown in [12,14], the approximate formula gives 10% error; therefore the direct calculation of the $1s$ level shift and width of kaonic hydrogen is desirable.

The observables given by the potential, together with the corresponding experimental data, are shown in Table II. It is seen that the $1s$ level shift $^1\Delta E_{1s}^{K^-p}$ and width $\Gamma_{1s}^{K^-p}$ of kaonic hydrogen of the $V_{\bar{K}N-\pi\Sigma-\pi\Lambda}^{\text{Chiral}}$ potential are in agreement with the most recent experimental data of the SIDDHARTA Collaboration [15]. Comparing the data in Table II with those from Table II of [2] we see that the chirally-motivated potential $V_{\bar{K}N-\pi\Sigma-\pi\Lambda}^{\text{Chiral}}$ gives a $1s$ level shift $\Delta E_{1s}^{K^-p}$ and width $\Gamma_{1s}^{K^-p}$ of kaonic hydrogen that are close to the results of the one-pole $V_{\bar{K}N-\pi\Sigma}^{1,\text{SIDD}}$ and the two-pole $V_{\bar{K}N-\pi\Sigma}^{2,\text{SIDD}}$ versions of the phenomenological potential. The chirally-motivated potential also reproduces the rather accurately measured threshold branching ratios γ , R_c , and R_n :

$$\gamma = \frac{\Gamma(K^-p \rightarrow \pi^+\Sigma^-)}{\Gamma(K^-p \rightarrow \pi^-\Sigma^+)}, \quad (5)$$

$$R_c = \frac{\Gamma(K^-p \rightarrow \pi^+\Sigma^-, \pi^-\Sigma^+)}{\Gamma(K^-p \rightarrow \text{all inelastic channels})}, \quad (6)$$

$$R_n = \frac{\Gamma(K^-p \rightarrow \pi^0\Lambda)}{\Gamma(K^-p \rightarrow \text{neutral states})}. \quad (7)$$

The medium value of the threshold branching ratio γ and of $R_{\pi\Sigma}$ constructed from R_c and R_n (see Eqs. (7) and (10) of [2]) are reproduced by the phenomenological potential as well; therefore, we can say that all three potentials reproduce the experimental data equally well.

The same is true for the elastic and inelastic K^-p cross sections $K^-p \rightarrow K^-p$, $K^-p \rightarrow \bar{K}^0n$, $K^-p \rightarrow \pi^+\Sigma^-$, $K^-p \rightarrow \pi^-\Sigma^+$, and $K^-p \rightarrow \pi^0\Sigma^0$. To demonstrate that all three potentials reproduce the cross sections with the same accuracy, we plotted the results of $V_{\bar{K}N-\pi\Sigma-\pi\Lambda}^{\text{Chiral}}$, $V_{\bar{K}N-\pi\Sigma}^{1,\text{SIDD}}$ and $V_{\bar{K}N-\pi\Sigma}^{2,\text{SIDD}}$ interaction models in the same figure (see Fig. 1). The experimental data in the figure are taken from [18–22]. As was

¹We define the $1s$ level shift as $\Delta E_{1s} = E_{1s}^{\text{Coul}} - \text{Re}(E_{1s}^{S+\text{Coul}})$, where E_{1s}^{Coul} is the energy calculated with the Coulomb interaction only.

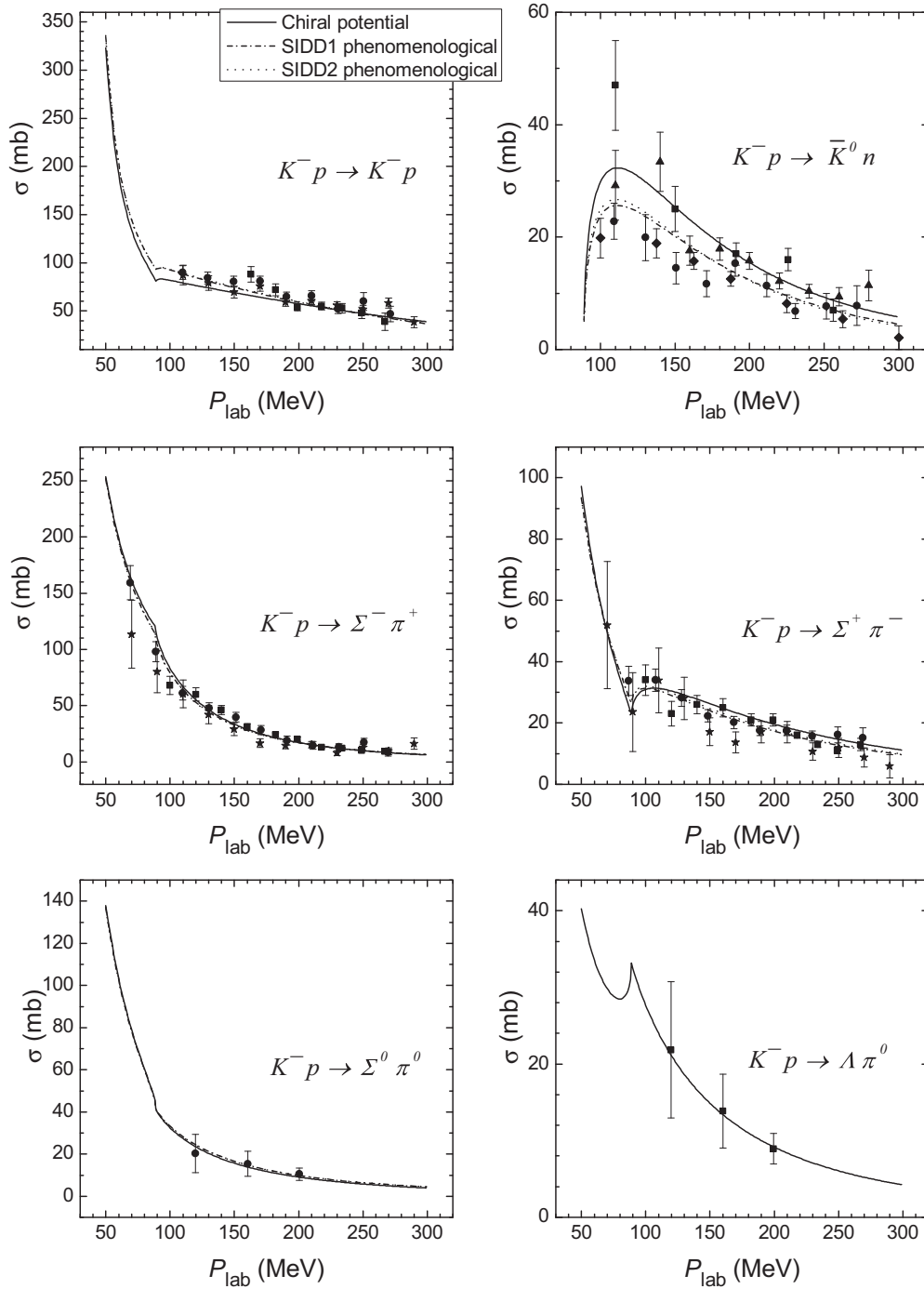


FIG. 1. Comparison of the elastic and inelastic K^-p cross sections for the chirally-motivated potential $V_{\bar{K}N-\pi\Sigma}^{\text{Chiral}}$ (solid lines) with the one-pole $V_{\bar{K}N-\pi\Sigma}^{1,\text{SIDD}}$ (dash-dotted lines) and two-pole $V_{\bar{K}N-\pi\Sigma}^{2,\text{SIDD}}$ (dotted lines) phenomenological potentials from [2]. The experimental data are taken from [18–22] (data points).

done previously, one set of data [23] is neglected owing to large experimental errors.

Unlike most of the authors of models of the $\bar{K}N$ interaction we need not know the K^-p scattering length a_{K^-p} to calculate the characteristics of kaonic hydrogen. However, we can calculate it directly from the $V_{\bar{K}N-\pi\Sigma-\pi\Lambda}^{\text{Chiral}}$ potential: its value is

$$a_{K^-p} = -0.77 + i 0.84 \text{ fm.} \quad (8)$$

The isospin-diagonal $I = 0$ and $I = 1$ $\bar{K}N$ scattering lengths

$$a_{\bar{K}N,0} = -1.65 + i 1.26 \text{ fm}, \quad a_{\bar{K}N,1} = 0.52 + i 0.48 \text{ fm} \quad (9)$$

are not connected with the a_{K^-p} value by the simple formula $a_{K^-p} = (a_{\bar{K}N,0} + a_{\bar{K}N,1})/2$ since physical masses are used whereas the $V_{\bar{K}N-\pi\Sigma-\pi\Lambda}^{\text{Chiral}}$ potential is constructed together with the isospin-nonconserving Coulomb interaction. In the three-body AGS equations, however, isospin-averaged masses are

used, which lead to different values of the scattering lengths:

$$a_{K^-p}^{\text{aver}} = -0.49 + i 0.71 \text{ fm}, \quad (10)$$

$$a_{\bar{K}N,0}^{\text{aver}} = -1.50 + i 0.84 \text{ fm}, \quad (11)$$

$$a_{\bar{K}N,1}^{\text{aver}} = 0.53 + i 0.59 \text{ fm}.$$

In the same way as other chirally-motivated potentials, our new potential has two strong poles for the $\Lambda(1405)$ resonance:

$$z_1 = 1417 - i 33 \text{ MeV}, \quad z_2 = 1406 - i 89 \text{ MeV}. \quad (12)$$

Both are situated on the proper Riemann sheets, corresponding to a resonance in the $\pi\Sigma$ channel and a quasi-bound state in the $\bar{K}N$ channel. They are connected to the $\pi\Lambda$ channel too through isospin-nonconserving parts. The real parts of the poles are situated between the $\bar{K}N$ and $\pi\Sigma$ thresholds as one would expect. Because of the above-mentioned isospin mixing the poles z_1 and z_2 are not pure $I = 0$ states. They have a small admixture of the isospin $I = 1$ state (see [14] for details). The two-pole structure of the $\Lambda(1405)$ resonance follows from the energy-dependent form of the potential. To achieve the same property of our two-pole phenomenological potential $V_{\bar{K}N-\pi\Sigma}^{2,\text{SIDD}}$ we used a more complicated form factor in the $\pi\Sigma$ channel.

In the same way as in [14] we checked where the poles move when the nondiagonal couplings of the potential were gradually reduced to zero. The results are demonstrated in Fig. 2. It is seen that the strong pole z_1 becomes a real bound state with smaller than the original binding energy when the $\bar{K}N$, $\pi\Sigma$, and $\pi\Lambda$ channels are uncoupled. The second strong pole z_2 remains a resonance pole, situated between the $\bar{K}N$ and $\pi\Sigma$ channels, but with smaller real and larger imaginary parts. The same trajectory drawn for the $1s$ level shift and width of kaonic hydrogen (see Fig. 3) shows that the pole, corresponding to the atomic state, also becomes a real bound state. The $1s$ level shift is large for the decoupled system.

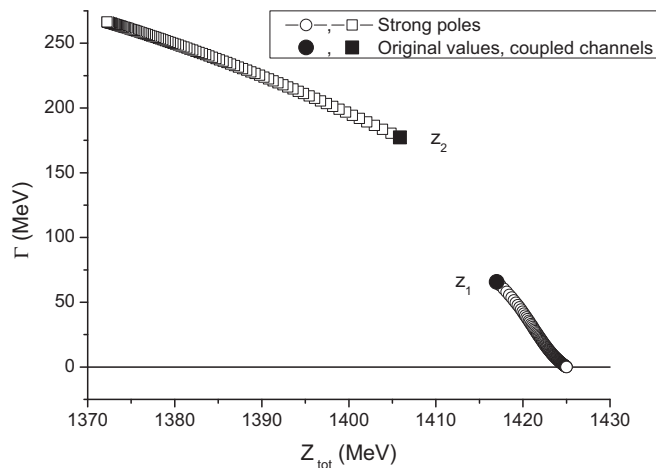


FIG. 2. Trajectories of the strong poles when the coupling between the $\bar{K}N$, $\pi\Sigma$, and $\pi\Lambda$ channels is gradually being switched off (empty symbols). The filled symbols denote the original values with coupled channels.

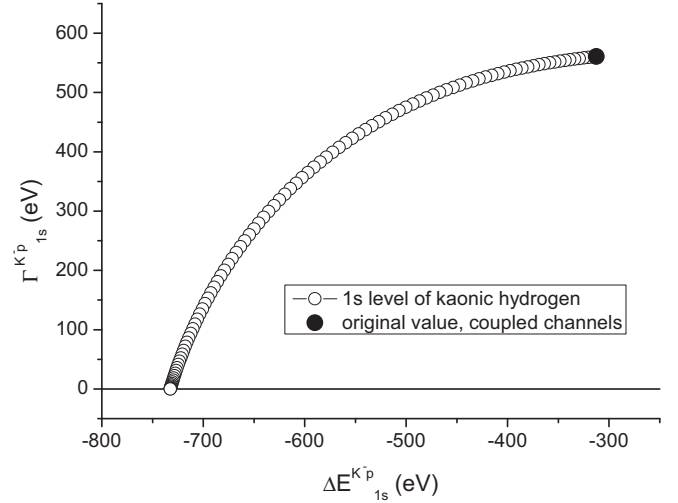


FIG. 3. The same as Fig. 2 for the $1s$ level of kaonic hydrogen.

Theoretically, the $\Lambda(1405)$ resonance peak could be seen in the elastic $\pi^0\Sigma^0$ cross sections; however, the corresponding experimental peak can be observed only as an Final State Interaction (FSI) peak in a more complicated reaction involving three or more particles. In this case the virtual $\bar{K}N \rightarrow \pi\Sigma$ process can also contribute to the $\pi\Sigma$ yield in a final state. The extent of this contribution can be reliably determined only by considering the complete, rather complicated process (see, e.g., Eq. (11) in [24]). Instead, many authors of $\bar{K}N$ interaction models add the $\bar{K}N \rightarrow \pi\Sigma$ amplitude to the $\pi\Sigma \rightarrow \pi\Sigma$ one and introduce an adjustable parameter in front of it to compare the theoretical predictions with experimental $\pi\Sigma$ missing mass spectra. The corresponding cross sections are multiplied by the $\pi\Sigma$ relative momentum, which is a phase space factor coming from the FSI formalism. We did not follow that routine and demonstrate the effect of the $\Lambda(1405)$ resonance in elastic $\pi^0\Sigma^0$ cross sections (see Fig. 4).

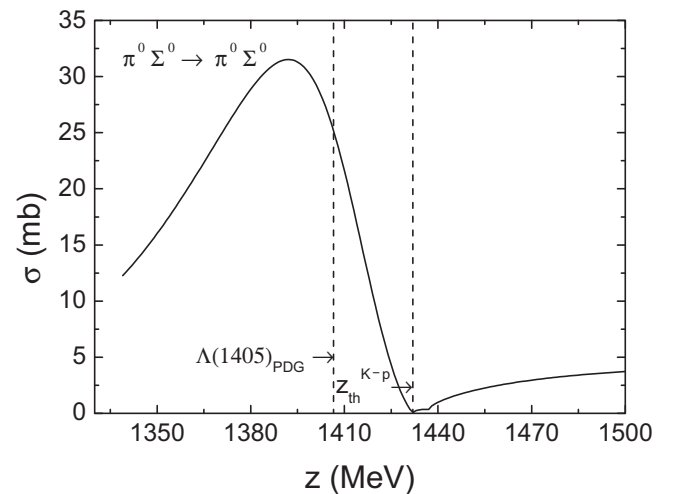


FIG. 4. Elastic $\pi^0\Sigma^0$ cross sections of the chirally-motivated potential $V_{\bar{K}N-\pi\Sigma-\pi\Lambda}^{\text{Chiral}}$. The Particle Data Group value for the mass of the $\Lambda(1405)$ resonance and the K^-p threshold are also shown.

TABLE III. Scattering lengths of K^-d scattering, a_{K^-d} (in fm), and effective range $r_{K^-d}^{\text{eff}}$ (in fm) obtained from AGS calculations with the chirally-motivated $V_{\bar{K}N-\pi\Sigma-\pi\Lambda}^{\text{Chiral}}$ potential (3) and the one-pole $V_{\bar{K}N-\pi\Sigma}^{1,\text{SIDD}}$ and two-pole $V_{\bar{K}N-\pi\Sigma}^{2,\text{SIDD}}$ phenomenological potentials from [2]. K^-d scattering length values from other Faddeev calculations are also shown. The $1s$ level shift $\Delta E_{1s}^{K^-d}$ (eV) and width $\Gamma_{1s}^{K^-d}$ (eV) of kaonic deuterium, calculated using the three potentials, are shown as well.

	a_{K^-d}	$r_{K^-d}^{\text{eff}}$	$\Delta E_{1s}^{K^-d}$	$\Gamma_{1s}^{K^-d}$
AGS with $V_{\bar{K}N-\pi\Sigma-\pi\Lambda}^{\text{Chiral}}$ (this work)	$-1.59 + i 1.32$	$0.50 - i 1.17$	-828	1055
AGS with $V_{\bar{K}N-\pi\Sigma}^{1,\text{SIDD}}$ [2]	$-1.49 + i 1.24$	$0.69 - i 1.31$	-785	1018
AGS with $V_{\bar{K}N-\pi\Sigma}^{2,\text{SIDD}}$ [2]	$-1.51 + i 1.25$	$0.69 - i 1.34$	-797	1025
MFST [6]	$-1.58 + i 1.37$			
Deloff [5]	$-0.85 + i 1.05$			
TDD [4]	$-1.34 + i 1.04$			
TGE [3]	$-1.47 + i 1.08$			

III. K^-d ELASTIC SCATTERING AND THE K^-d QUASI-BOUND STATE

We solved Faddeev-type equations in Alt-Grassberger-Sandhas form for the $\bar{K}NN$ system with the coupled $\pi\Sigma N$ channel, which for the N -term isospin-dependent separable potentials

$$V_{i,I}^{\alpha\beta} = \sum_{m=1}^{N_i^\alpha} \lambda_{i(m),I}^{\alpha\beta} |g_{i(m),I}^\alpha\rangle \langle g_{i(m),I}^\beta| \quad (13)$$

is the system of equations for the unknown operators $X_{ij,I_i I_j}^{\alpha\beta}$:

$$X_{i(l)j,I_i I_j}^{\alpha\beta} = \delta_{\alpha\beta} \sum_{m=1}^{N_j^\alpha} C_{j(m)}^\alpha Z_{i(l)j(m),I_i I_j}^\alpha + \sum_{k,\gamma=1}^3 \sum_{m,n=1}^{N_k^\alpha} \sum_{I_k} Z_{i(l)k(m),I_i I_k}^\alpha \tau_{k(mn),I_k}^{\alpha\gamma} X_{k(n)j,I_k I_j}^{\gamma\beta}. \quad (14)$$

The ‘‘particle channel’’ indices $\alpha, \beta = 1, 2, 3$ are used in Eqs. (13) and (14) additionally to the usual Faddeev partition indices $i, j, k = 1, 2, 3$. The N_i^α in the equations is the number of terms of the separable potential, λ is a strength constant, and g is a form factor. The function $\tau_{k(mn),I_k}^{\alpha\gamma}$ is the energy-dependent part of the T matrix of the separable potential (13). Additional details of the formulas can be found in our previous paper [1]. The equations properly describe the three-body dynamics of the system. They are written in momentum representation, and isospin formalism is used. The equations were properly antisymmetrized, which is necessary because there are two baryons in every channel. The logarithmic singularities in the kernels of the equations were treated by the method suggested in [25]. The three-body calculations were performed without taking the Coulomb interaction into account since its effect is expected to be small.

The elastic K^-d amplitudes, including the scattering length, and effective range were calculated by using the chirally-motivated $V_{\bar{K}N-\pi\Sigma-\pi\Lambda}^{\text{Chiral}}$ potential described in the previous section. We used averaged masses in the potential as well as in the the whole three-body calculation since it was shown in [24] that the effect of physical masses is rather small.

The three-channel $\bar{K}N-\pi\Sigma-\pi\Lambda$ potential was used in the $\bar{K}NN-\pi\Sigma N$ AGS equations in the form of the exact optical two-channel $\bar{K}N-\pi\Sigma(-\pi\Lambda)$ potential, when the $\bar{K}N-\bar{K}N$, $\bar{K}N-\pi\Sigma$, and $\pi\Sigma-\pi\Sigma$ elements of the three-channel T matrix are used as the two-channel T matrix. The remaining two-body potentials, needed for the three-body calculation, are also separable. The two-term TSA-B NN and the exact optical $\Sigma N(-\Lambda N)$ potentials that were used are described in [1]. The NN interaction model reproduces the phase shifts of the Argonne V18 potential and is therefore repulsive at short distances. It gives the proper NN scattering length, effective range, and binding energy of the deuteron. The two-channel $\Sigma N-\Lambda N$ potential reproduces the experimental ΣN and ΛN cross sections, while the corresponding exact optical $\Sigma N(-\Lambda N)$ potential has exactly the same elastic ΣN amplitude as the two-channel potential.

The K^-d scattering length a_{K^-d} obtained with the chirally-motivated potential is shown in Table III. The new three-body result is compared to those from [2] with one-pole $V_{\bar{K}N-\pi\Sigma}^{1,\text{SIDD}}$ and two-pole $V_{\bar{K}N-\pi\Sigma}^{2,\text{SIDD}}$ versions of the phenomenological $\bar{K}N$ potential. The ‘‘phenomenological’’ results in the table differ slightly from the three-body values from Table II of [2] since here we used the spin-independent $\Sigma N(-\Lambda N)$ potential, while the spin-dependent potential was used in the previous paper. It is seen that the chirally-motivated potential leads to about 6% larger absolute value of the real and imaginary parts of the scattering length. The difference is quite small, so we can conclude that the three different models of the $\bar{K}N$ interaction, which reproduce low-energy data on K^-p scattering and kaonic hydrogen with the same level of accuracy, give quite similar results for low-energy K^-d scattering.

Since it was shown [1] that the fixed scatterer approximation (also called the fixed center approximation) gives error of about 30% for the K^-d scattering length, this time we do not compare the results obtained with this method with ours. Four a_{K^-d} values obtained in other Faddeev calculations are shown in Table III. Comparing to them, we see that the result of the very recent calculation with coupled channels [6] gives the real part of a_{K^-d} that almost coincides with our result for the chirally-motivated potential. The imaginary part of the K^-d scattering length from [6] is slightly larger, which can follow from the fact that the $\bar{K}N$ interaction model used there was fitted to kaonic

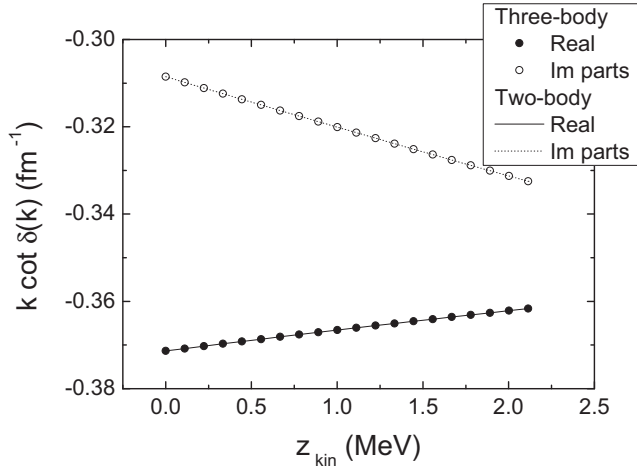


FIG. 5. The elastic near-threshold K^-d amplitudes presented in the form of a $k \cot \delta(k)$ function. Real (filled circles) and imaginary (empty circles) parts of the functions obtained from the coupled-channel three-body AGS equations using the chirally motivated potential $V_{\bar{K}N-\pi\Sigma-\pi\Lambda}^{\text{Chiral}}$ are shown. The two-body results obtained with the complex $\bar{K}^- - d$ potential are demonstrated as well (by a solid line for the real part and a dotted line for the imaginary part of the function).

hydrogen data not directly but through the K^-p scattering length and the approximate formula, which is the least reliable just in reproducing the imaginary part of the level shift.

The one-channel result of the Faddeev calculation [5] lies far away from all the others. Two effects play a role here: one-channel dynamics and, therefore, indirectly taking the $\pi\Sigma N$ channel into account and problems with reproducing experimental data by the complex potential, used in the paper. It was demonstrated in [1] for phenomenological models of the $\bar{K}N$ interaction that simple complex potentials have quite large error, whereas an exact optical $\bar{K}N$ potential gives rather an accurate result for the scattering length. The exact optical potential with $\bar{K}N$ amplitudes exactly corresponding to those from the potential with coupled channels is good for the chirally-motivated model as well. It gives

$$a_{K^-d}^{\text{Chiral,Opt}} = -1.57 + i 1.32 \text{ fm}, \quad (15)$$

which is very close to the coupled-channel result from Table III.

Finally, two old a_{K^-d} values [3,4] significantly underestimate the imaginary part of the K^-d scattering length.

We also calculated the effective range $r_{K^-d}^{\text{eff}}$ of K^-d scattering; the results can be seen in Table III. The real part of $r_{K^-d}^{\text{eff}}$ of the chirally-motivated potential is much smaller than those of our phenomenological potentials. The imaginary part is smaller by the absolute value. Near-threshold elastic amplitudes of K^-d scattering are needed for construction of a complex two-body $K^- - d$ potential and further calculation of the $1s$ level of kaonic deuterium. They are presented in $k \cot \delta(k)$ form in Fig. 5.

The relative values of $|\text{Re} a_{K^-d}|$ and $|\text{Im} a_{K^-d}|$ obtained with each one of our three potentials together with their signs

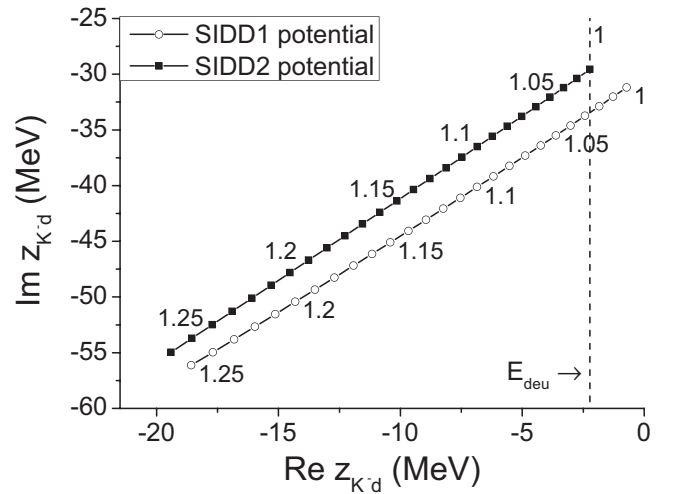


FIG. 6. Pole trajectories in the K^-d system for increasing absolute value of the $\lambda_{I=0}^{\bar{K}\bar{K}}$ strength constant of the phenomenological $V_{\bar{K}N-\pi\Sigma}^{1,\text{SIDD}}$ and $V_{\bar{K}N-\pi\Sigma}^{2,\text{SIDD}}$ potentials. The numbers along the trajectories indicate the multiplication factors. The position of the K^-d threshold is also shown; quasi-bound states are the poles to the left of it.

might lead to the conclusion that a bound or a quasi-bound state could exist in the K^-d system. Indeed, a simple analytical continuation of the effective range formula below the K^-d threshold suggests a K^-d quasi-bound state at $-14.6 - i 11.0$ MeV for the chirally-motivated potential $V_{\bar{K}N-\pi\Sigma-\pi\Lambda}^{\text{Chiral}}$, at $-19.6 - i 8.2$ MeV for $V_{\bar{K}N-\pi\Sigma}^{1,\text{SIDD}}$, and at $-18.9 - i 7.8$ MeV for the $V_{\bar{K}N-\pi\Sigma}^{2,\text{SIDD}}$ potential (with the real parts being measured from the K^-d threshold). A systematic search for these quasi-bound states based on the AGS equations (the details of which are described in our next paper [26] devoted to the K^-pp system) did not find them, either in the neighborhood of these predictions or elsewhere.² The reason must be the validity of the effective range formula, which is limited to the vicinity of the corresponding threshold. Since the K^-d state is expected to have a rather large width (similarly to the K^-pp case), it is definitely out of such a region. The only $\bar{K}N$ potential that gives a quasi-bound state in the K^-d system is one of our older phenomenological potentials [1], which does not reproduce SIDDHARTA data but reproduces KEK data on kaonic hydrogen [27] only.

We checked, whether the absence of a K^-d quasi-bound state is caused by the insufficient attraction in the $\bar{K}N$ channel with $I = 0$, which is believed to be less important in the K^-d system than $\bar{K}N$ with $I = 1$. Namely, we performed a series of calculations where the $\lambda_{I=0}^{\bar{K}\bar{K}}$ strength constants of our phenomenological potentials $V_{\bar{K}N-\pi\Sigma}^{1,\text{SIDD}}$ and $V_{\bar{K}N-\pi\Sigma}^{2,\text{SIDD}}$ were multiplied by some factor. For the chirally-motivated model such a procedure is more complicated, since there the relative strength of the $I = 0$ and $I = 1$ interaction is fixed. The results are shown in Fig. 6, which demonstrates that increasing of the

²Obviously, we identify poles as quasi-bound states in the K^-d system if their real parts are situated between the $\pi\Sigma N$ and K^-d thresholds.

absolute value of the $\lambda_{I=0}^{\vec{k}\vec{k}}$ strength constant and, therefore, of the attraction in the $I = 0$ $\bar{K}N$ subsystem leads to the appearance of K^-d quasi-bound states.

IV. CHARACTERISTICS OF KAONIC DEUTERIUM

Our aim was to calculate a physical quantity that characterizes the low-energy properties of the K^-d system and can be compared to experimental data directly. The scattering length is not of this type, while the $1s$ level shift and width of kaonic deuterium can be measured. Therefore, we calculated these atomic observables, which correspond to the results of our three-body calculations of low-energy K^-d scattering.

Since performing the Faddeev calculation with the Coulomb plus a strong interaction is too hard, a two-body calculation with a complex $K^- - d$ potential was performed instead. The potential is a separable one with two terms,

$$V_{K^-d}(\vec{k}, \vec{k}') = \lambda_{1,K^-d} g_1(\vec{k}) g_1(\vec{k}') + \lambda_{2,K^-d} g_2(\vec{k}) g_2(\vec{k}'), \quad (16)$$

and Yamaguchi form factors

$$g_i(k) = \frac{1}{\beta_{i,K^-d}^2 + k^2}, \quad i = 1, 2. \quad (17)$$

The parameters of the potential,

$$\beta_{1,K^-d} = 1.5 \text{ fm}^{-1}, \quad \lambda_{1,K^-d} = -0.0628 - i 0.4974 \text{ fm}^{-2}, \quad (18)$$

$$\beta_{2,K^-d} = 1.1, \text{ fm}^{-1}, \quad \lambda_{2,K^-d} = -0.1123 + i 0.1556 \text{ fm}^{-2}, \quad (19)$$

were fixed by fitting the near-threshold three-body K^-d amplitudes calculated using the AGS equations, described in the previous section. The result of the fit can be seen in Fig. 5, where the $k \cot \delta(k)$ functions calculated using the complex $K^- - d$ potential are plotted as solid (real part) and dotted (imaginary part) lines. Comparing the lines with the corresponding dots, denoting the three-body results, we see that the description is excellent. Obviously, the potential (16) reproduces the scattering length a_{K^-d} and effective range $r_{K^-d}^{\text{eff}}$ from Table III.

The Lippmann-Schwinger equation with the complex $K^- - d$ and pointlike Coulomb potentials was then solved and the $1s$ level energy was obtained. Additional details about the calculation can be found in [2,14]. The shift $\Delta E_{1s}^{K^-d}$ and width $\Gamma_{1s}^{K^-d}$ of kaonic deuterium, corresponding to the chirally-motivated model of the $\bar{K}N-\pi\Sigma-\pi\Lambda$ interaction, are shown in Table III. We also show the characteristics of the atom, obtained with our phenomenological potentials $V_{\bar{K}N-\pi\Sigma}^{1,\text{SIDD}}$ and $V_{\bar{K}N-\pi\Sigma}^{2,\text{SIDD}}$ [2].

The ‘‘chirally-motivated’’ absolute values of the level shift $\Delta E_{1s}^{K^-d}$ and the width $\Gamma_{1s}^{K^-d}$ are both larger than those obtained in [2] for the phenomenological $\bar{K}N-\pi\Sigma$ potentials. In view of the results for the K^-d scattering lengths discussed in the previous section, this is an expected result since the $1s$ level shift and width of a hadronic atom are directly connected to the strong scattering length of the system. However, the results obtained using three different models of the $\bar{K}N$ interaction are rather close to each other. We think that the important point

here is the fact that all three potentials reproduce low-energy experimental data on K^-p scattering and kaonic hydrogen with the same level of accuracy.

We checked the accuracy of the approximate corrected Deser formula, allowing simple computation of characteristics of a kaonic atom from a known scattering length. The result obtained using the a_{K^-d} value from Table III,

$$\Delta E_{K^-d,cD}^{\text{Chiral}} = -878 \text{ eV}, \quad \Gamma_{K^-d,cD}^{\text{Chiral}} = 724 \text{ eV}, \quad (20)$$

compared to the more accurate ones $\Delta E_{K^-d}^{\text{Chiral}}$ and $\Gamma_{K^-d}^{\text{Chiral}}$ from the same table show that in this case the error of the approximate formula is as large as for the case of phenomenological $\bar{K}N$ potentials. As in [2], the corrected Deser formula underestimates the width of the $1s$ level of kaonic deuterium by 30%. Therefore, the validity of this statement does not depend on the model of the $\bar{K}N$ interaction.

We would like to note that our results for $\Delta E_{K^-d}^{\text{Chiral}}$ and $\Gamma_{K^-d}^{\text{Chiral}}$, shown in Table III, cannot be called ‘‘exact,’’ but only ‘‘accurate’’ since the $1s$ level shift and width were obtained from the two-body calculation with a pointlike deuteron interacting with a kaon through the complex potential. This means that the size of the deuteron was taken into account only effectively through the potential, which reproduces the three-body K^-d AGS amplitudes. As for the corrected Deser formula, it contains no three-body information at all since the only input is a K^-d scattering length. Moreover, the formula relies on further approximations, which are absent in our calculation, and gives a 10% error already for the two-body case.

V. CONCLUSIONS

We constructed a three-channel isospin-dependent chirally-motivated $\bar{K}N-\pi\Sigma-\pi\Lambda$ potential and used it in the Faddeev-type calculations of the low-energy elastic K^-d amplitudes, including K^-d scattering length, and effective range. The potential reproduces all low-energy experimental data on K^-p scattering and characteristics of kaonic hydrogen with the same level of accuracy as our phenomenological potentials with one- and two-pole structure of the $\Lambda(1405)$ resonance. Comparison of the results allows to reveal the effect of the three different models of the $\bar{K}N$ interaction used in the three-body calculations. It turns out that the low-energy K^-d elastic amplitudes and characteristics of kaonic deuterium obtained with the three potentials are rather close to each other. Therefore, comparison with eventual experimental results on kaonic deuterium hardly could distinguish these models of the $\bar{K}N$ interaction. Additionally, we found no quasi-bound states in the K^-d system and, for the phenomenological potentials shown, this lack of quasi-bound states is caused by insufficient attraction in the $I = 0$ $\bar{K}N$ subsystem.

ACKNOWLEDGMENTS

The work was supported by the Czech GACR Grant No. P203/12/2126 and the Hungarian OTKA Grant No. 109462. One of the authors (N.V.S.) is grateful to J. Haidenbauer for his comments on some details of $\bar{K}N$ models of interaction.

- [1] N. V. Shevchenko, *Phys. Rev. C* **85**, 034001 (2012).
- [2] N. V. Shevchenko, *Nucl. Phys. A* **890–891**, 50 (2012).
- [3] G. Toker, A. Gal, and J. M. Eisenberg, *Nucl. Phys. A* **362**, 405 (1981).
- [4] M. Torres, R. H. Dalitz, and A. Deloff, *Phys. Lett. B* **174**, 213 (1986).
- [5] A. Deloff, *Phys. Rev. C* **61**, 024004 (2000).
- [6] T. Mizutani, C. Fayard, B. Saghai, and K. Tsushima, *Phys. Rev. C* **87**, 035201 (2013).
- [7] C. Curceanu *et al.*, *Nucl. Phys. A* **914**, 251 (2013).
- [8] B. Borasoy, U.-G. Meißner, and R. Nißler, *Phys. Rev. C* **74**, 055201 (2006).
- [9] A. Cieplý and J. Smejkal, *Nucl. Phys. A* **881**, 115 (2012).
- [10] Z.-H. Guo and J. A. Oller, *Phys. Rev. C* **87**, 035202 (2013).
- [11] Y. Ikeda, T. Hyodo, and W. Weise, *Nucl. Phys. A* **881**, 98 (2012).
- [12] A. Cieplý and J. Smejkal, *Eur. Phys. J. A* **34**, 237 (2007).
- [13] U.-G. Meißner, U. Raha, and A. Rusetsky, *Eur. Phys. J. C* **35**, 349 (2004).
- [14] J. Révai and N. V. Shevchenko, *Phys. Rev. C* **79**, 035202 (2009).
- [15] M. Bazzi *et al.* (SIDDHARTA Collaboration), *Phys. Lett. B* **704**, 113 (2011).
- [16] D. N. Tovee *et al.*, *Nucl. Phys. B* **33**, 493 (1971).
- [17] R. J. Nowak *et al.*, *Nucl. Phys. B* **139**, 61 (1978).
- [18] M. Sakitt *et al.*, *Phys. Rev.* **139**, B719 (1965).
- [19] J. K. Kim, *Phys. Rev. Lett.* **14**, 29 (1965); **19**, 1074 (1967).
- [20] W. Kittel, G. Otter, and I. Wacek, *Phys. Lett.* **21**, 349 (1966).
- [21] J. Ciborowski *et al.*, *J. Phys. G* **8**, 13 (1982).
- [22] D. Evans *et al.*, *J. Phys. G* **9**, 885 (1983).
- [23] W. E. Humphrey and R. R. Ross, *Phys. Rev.* **127**, 1305 (1962).
- [24] J. Révai, *Few-Body Syst.* **54**, 1865 (2013).
- [25] F. Sohre and H. Ziegelman, *Phys. Lett. B* **34**, 579 (1971).
- [26] J. Révai and N. V. Shevchenko, following paper, *Phys. Rev. C* **90**, 034004 (2014).
- [27] T. M. Ito *et al.*, *Phys. Rev. C* **58**, 2366 (1998).